JOURNAL OF COMPUTATIONAL PHYSICS 92, 142–160 (1991)

Flux-Corrected Transport Techniques for Multidimensional Compressible Magnetohydrodynamics

C. RICHARD DEVORE

Laboratory for Computational Physics and Fluid Dynamics, Naval Research Laboratory, Washington, DC 20375-5000

Received July 19, 1989; revised October 25, 1989

A prescription is given for conservatively integrating generalized hydromagnetic equations using flux-corrected transport (FCT) techniques. By placing the magnetic-field components at the interface locations of the finite-difference grid, the field is kept divergence-free to within machine roundoff error. The use of FCT techniques allows an integration scheme of high accuracy to be employed, while the numerical ripples associated with large dispersion errors are avoided. The method is particularly well suited for problems involving magnetohydrodynamic shocks and other discontinuities.

1. INTRODUCTION

Flux-corrected transport (FCT) [1–9] was originally conceived, and has been developed over the years, as a method for accurately solving the conservation equations of Eulerian hydrodynamics without violating the positivity of mass and energy, particularly near shocks and other discontinuities. This is achieved by adding to the equations a strong numerical diffusion, which guarantees the positivity of the solution, followed by a compensating antidiffusion, which reduces the numerical error. The crux of the FCT method lies in limiting ("correcting") the antidiffusive fluxes before they are applied, so that no unphysical extrema are created in the solution. The effect of this flux-correction procedure is to provide as accurate a solution to the original equation as is consistent with maintaining positivity and monotonicity everywhere.

My objective in this paper is to give a prescription for integrating the hydromagnetic equation of magnetohydrodynamics (MHD) using FCT techniques. The application of FCT to this problem has been considered previously [2, 10], but no generally satisfactory procedure for correcting the antidiffusive fluxes, while simultaneously keeping the magnetic field divergence-free, has heretofore been established. Placing the discrete values of the field components at the interface locations of the spatial grid enables the divergence-free character of the magnetic field, as expressed by the discrete integral form of Gauss's law, to be simply and strictly preserved [11, 12]. The monotonicity constraint of FCT, on the other hand, cannot be strictly enforced without producing an excessively diffuse solution. I describe a

0021-9991/91 $3.00

flux-corrector which constructs the total antidiffusive flux as the sum of corrected partial fluxes. Each component of the magnetic field contributes a partial flux to the total, and its contribution is limited independently of those due to the other field components. The solutions so obtained have remained well behaved even in severe numerical test cases.

An efficient, accurate algorithm which uses these techniques to integrate generalized hydromagnetic equations in two spatial dimensions is described in the Appendix. The phase and amplitude errors of the solution are fourth order in the grid spacing at long wavelengths. I present and discuss some numerical examples using this new FCT algorithm and compare its performance with those of an alternative monotone scheme [12], which solves directly for the magnetic field, and a companion FCT algorithm [13], which solves for the vector potential.

2. TECHNIQUES

The conservation equations of Eulerian magnetohydrodynamics take the general form

$$\frac{\partial \rho}{\partial t} + \nabla \cdot (\rho \mathbf{v}) = s_1 + \mathbf{s}_2 \cdot \nabla s_3 + \nabla \cdot \mathbf{s}_4,$$
$$\frac{\partial \mathbf{B}}{\partial t} = \nabla \times (\mathbf{v} \times \mathbf{B}) + \nabla \times \mathbf{s}_5, \tag{1}$$

where ρ is a fluid variable (mass, momentum, or energy density) being time-advanced, $\mathbf{v}$ is the fluid velocity, $\mathbf{B}$ is the magnetic field, and s_1, $\mathbf{s}_2$, s_3, $\mathbf{s}_4$, and $\mathbf{s}_5$ are source terms. In the absence of sources, Eqs. (1) reduce to the continuity and ideal hydromagnetic equations,

$$\frac{\partial \rho}{\partial t} + \nabla \cdot (\rho \mathbf{v}) = 0,$$
$$\frac{\partial \mathbf{B}}{\partial t} = \nabla \times (\mathbf{v} \times \mathbf{B}). \tag{2}$$

The integral conservation relations corresponding to Eqs. (2) are

$$\frac{\partial}{\partial t} \int_\rho \rho \, dV = -\oint_S \rho \mathbf{v} \cdot d\mathbf{S},$$
$$\frac{\partial}{\partial t} \int_S \mathbf{B} \cdot d\mathbf{S} = \oint_C \mathbf{v} \times \mathbf{B} \cdot dl, \tag{3}$$

where in the first integral V is any volume of fluid bounded by the closed surface S, and in the second, S is any (open) surface bounded by the closed contour C.

The geometry of a finite-difference representation of Eqs. (1) is shown in Fig. 1. It has long been recognized that the continuity equation can be integrated conservatively by evaluating the flux densities $\rho\mathbf{v}$ at the interfaces of the spatial grid and using a discrete representation of the integral relation (3a). For example, a forward differencing of the time derivative and an explicit treatment of the spatial derivatives in two dimensions lead to

$$([\rho^c - \rho^o]\, V)_{ij}\, \Delta t^{-1} = (\rho^o v_x A_x)_{i-1/2j} - (\rho^o v_x A_x)_{i+1/2j} + (\rho^o v_y A_y)_{ij-1/2} - (\rho^o v_y A_y)_{ij+1/2}, \tag{4}$$

where ρ^o and ρ^c are the values of the fluid variable before and after the convection, respectively, V is the cell volume, A_x and A_y are the areas of interfaces normal to the x and y directions, and Δt is the time increment. In a summation of the results (4) over any collection of cells in the system, the contributions of fluxes evaluated at the common, internal interfaces cancel pairwise. The integral conservation relation (3a) in its discrete form then holds for every subvolume of the system. This result also holds for the generalized continuity equation (1a), if only conservative sources $\mathbf{s}_4$ are present.

A conservative integration of the hydromagnetic equation is similarly effected [11, 12] by placing the components of the magnetic field at the cell interfaces, as shown in the right panel of Fig. 1. The flux densities $\mathbf{v} \times \mathbf{B}$ are evaluated at the cell edges, and a discrete representation of the integral conservation relation (3b) again is used. If v_z and B_z both vanish, discretizing in time as before yields

$$\begin{aligned}([B_x^c - B_x^o]\, A_x)_{i+1/2j}\, \Delta t^{-1} &= ([v_y B_x^o - v_x B_y^o]\, L_z)_{i+1/2j-1/2} - ([v_y B_x^o - v_x B_y^o]\, L_z)_{i+1/2j+1/2}, \\ ([B_y^c - B_y^o]\, A_y)_{ij+1/2}\, \Delta t^{-1} &= ([v_x B_y^0 - v_y B_x^o]\, L_z)_{i-1/2j+1/2} - ([v_x B_y^o - v_y B_x^o]\, L_z)_{i+1/2j+1/2},\end{aligned} \tag{5}$$

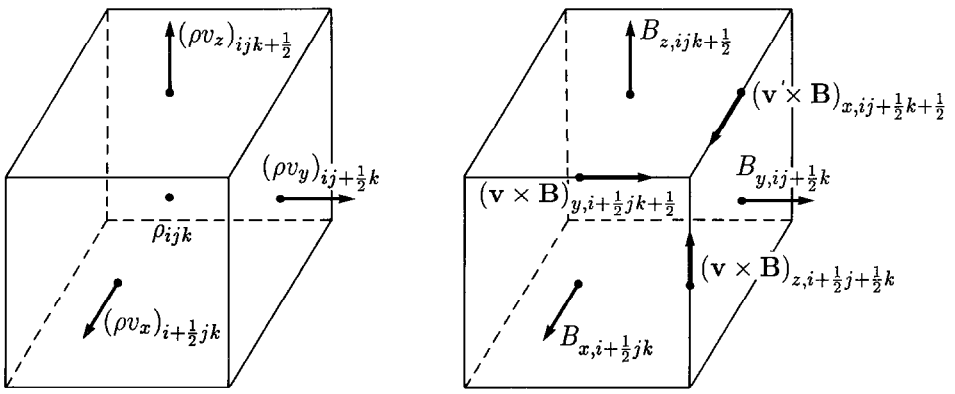

FIG. 1. Geometry of the finite-difference representations of the generalized continuity equations (left panel) and hydromagnetic equation (right panel) of conservative, Eulerian magnetohydrodynamics.

where $\mathbf{B}^o$ and $\mathbf{B}^c$ are the field values before and after the convection, and L_z is the length of an edge oriented in the z direction. Due to the pairwise cancellation of fluxes at common edges, the integral relation (3b) in its discrete form holds for any surface in the system. This result is also true of the generalized hydromagnetic equation (1b), whose conservative source term $\mathbf{s}_5$ is likewise evaluated at the cell edges. For the special case of a closed surface, all of the edge fluxes cancel and the solutions obey the discrete equivalent of

$$\frac{\partial}{\partial t} \oint_S \mathbf{B} \cdot d\mathbf{S} = 0. \tag{6}$$

Consequently, if Gauss's law in its discrete integral form is satisfied by the field configuration initially, it is satisfied for all time.

Thus, the conservation properties of both the generalized continuity and hydromagnetic equations (1) can be simply and strictly imposed on their discrete solutions by a judicious choice of the finite-difference representation used to solve them. A new algorithm for solving the hydromagnetic equation which exploits this representation in two spatial dimensions is described in the Appendix. The algorithm employs the techniques of flux-corrected transport (FCT) [1–9], which have been used extensively to solve problems in ordinary hydrodynamics. As noted originally by Book *et al.* [2], some difficulties arise in applying FCT to the hydromagnetic equation. These will now be addressed and a general resolution of them proposed.

The basic procedure for solving convective transport equations using FCT can be described as follows:

(1) Calculate a low-order-accurate but positive-definite solution (ρ^l, $\mathbf{B}^l$), by adding a strong numerical diffusion term to the equation.

(2) Calculate antidiffusive fluxes $\mathbf{F}^a$ which, if applied directly, would produce a high-order-accurate but potentially nonpositive and/or nonmonotonic solution (ρ^h, $\mathbf{B}^h$).

(3) "Correct" these antidiffusive fluxes, i.e., reduce them in magnitude, so that no unphysical extrema are created in the solution.

(4) Apply the corrected fluxes $\tilde{\mathbf{F}}^a$ to the low-order solution to obtain a more accurate, but still monotonic, final solution (ρ^f, $\mathbf{B}^f$).

The flux-correction step (3) is the key to the success of FCT. Zalesak's [5, 6] formulation of the flux-corrector for generalized continuity equations is the following:

(a) Establish the permitted extremal values of the solution in each cell. In two dimensions, e.g., a suitable choice might be

$$\begin{aligned} \tilde{\rho}_{ij} &= \max(\rho^o_{ij}, \rho^l_{ij}), \\ \rho^{\max}_{ij} &= \max(\tilde{\rho}_{i-1j-1}, \tilde{\rho}_{ij-1}, \tilde{\rho}_{i+1j-1}, \tilde{\rho}_{i-1j}, \tilde{\rho}_{ij}, \tilde{\rho}_{i+1j}, \tilde{\rho}_{i-1j+1}, \tilde{\rho}_{ij+1}, \tilde{\rho}_{i+1j+1}), \end{aligned} \tag{7}$$

with analogous expressions used to calculate $\rho^{\min}_{ij}$.

(b) Cancel those antidiffusive fluxes that are directed downstream with respect to the local gradient, i.e., which act to smooth the profile rather than steepen it. Thus, set

$$F^a_{x\ i+1/2j}=0 \qquad \text{if} \quad F^a_{x\ i+1/2j}(\rho^l_{i+1j}-\rho^l_{ij})<0$$

and

$$F^a_{x\ i+1/2j}(\rho^l_{i+2j}-\rho^l_{i+1j})<0 \tag{8}$$

or

$$F^a_{x\ i+1/2j}(\rho^l_{ij}-\rho^l_{i-1j})<0.$$

Such fluxes contribute to the formation of dispersive ripples, degrading the quality of the solution.

(c) Calculate the total inward- and outward-going antidiffusive fluxes for each cell,

$$\begin{aligned} P^+_{ij} &= \max(F^a_{x\ i-1/2j}, 0)-\min(F^a_{x\ i+1/2j}, 0) \\ &\quad +\max(F^a_{y\ ij-1/2}, 0)-\min(F^a_{y\ ij+1/2}, 0), \\ P^-_{ij} &= \max(F^a_{x\ i+1/2j}, 0)-\min(F^a_{x\ i-1/2j}, 0) \\ &\quad +\max(F^a_{y\ ij+1/2}, 0)-\min(F^a_{y\ ij-1/2}, 0). \end{aligned} \tag{9}$$

(d) Determine the maximum fractions of these fluxes which can be applied without causing overshoots or undershoots in the solution,

$$\begin{aligned} R^+_{ij} &= \min(1, Q^+_{ij}/P^+_{ij}), \\ R^-_{ij} &= \min(1, Q^-_{ij}/P^-_{ij}), \end{aligned} \tag{10}$$

where the maximum allowed fluxes into and out of the cell, respectively, are

$$\begin{aligned} Q^+_{ij} &= (\rho^{\max}_{ij}-\rho^l_{ij})\,V_{ij}, \\ Q^-_{ij} &= (\rho^l_{ij}-\rho^{\min}_{ij})\,V_{ij}. \end{aligned} \tag{11}$$

(e) At each interface, find the minimum fraction which prevents both an overshoot in the cell downstream from the flux and an overshoot in the cell upstream, viz.,

$$C_{x\ i+1/2j}=\begin{cases}\min(R^+_{i+1j}, R^-_{ij}), & \text{if} \quad F^a_{x\ i+1/2j}\geqslant 0; \\ \min(R^+_{ij}, R^-_{i+1j}), & \text{otherwise.}\end{cases} \tag{12}$$

(f) Finally, reduce the antidiffusive flux at the interface by this fraction,

$$\tilde{F}^a_{x\ i+1/2j}=C_{x\ i+1/2j}F^a_{x\ i+1/2j}. \tag{13}$$

In principle, Zalesak's flux-corrector for the continuity equation could be applied straightforwardly to the integration of the hydromagnetic equation. Steps (a)–(c) would be performed at each interface for the associated normal field component, and (d) and (e) at each edge, with the minimum taken over the upstream and downstream interfaces along both coordinate directions simultaneously. The solution which results is guaranteed to be monotonic, but it also is excessively diffuse, in practice. The difficulty originates in the mathematical form of the antidiffusive fluxes, the dominant, velocity-independent portion of which can be written symbolically as (see the Appendix)

$$F_z^a = \mu_{xx} \frac{\partial B_y}{\partial x} - \mu_{yy} \frac{\partial B_x}{\partial y}. \tag{14}$$

It is used to evolve the field components according to

$$\begin{aligned} \frac{\partial B_x}{\partial t} &= +\frac{\partial F_z^a}{\partial y} \\ &= -\frac{\partial}{\partial y} \mu_{yy} \frac{\partial B_x}{\partial y} + \frac{\partial}{\partial y} \mu_{xx} \frac{\partial B_y}{\partial x}, \\ \frac{\partial B_y}{\partial t} &= -\frac{\partial F_z^a}{\partial x} \\ &= -\frac{\partial}{\partial x} \mu_{xx} \frac{\partial B_y}{\partial x} + \frac{\partial}{\partial x} \mu_{yy} \frac{\partial B_x}{\partial y}. \end{aligned} \tag{15}$$

The first contributions on the right side of Eqs. (15) are clearly "antidiffusive" in character. The second contributions are not, unless the antidiffusivities μ are spatially uniform and the derivatives can be interchanged. In that case, $\nabla \cdot \mathbf{B} = 0$ can be used to obtain the antidiffusion equations

$$\begin{aligned} \frac{\partial B_x}{\partial t} &= -\mu_{yy} \frac{\partial^2 B_x}{\partial y^2} - \mu_{xx} \frac{\partial^2 B_x}{\partial x^2}, \\ \frac{\partial B_y}{\partial t} &= -\mu_{xx} \frac{\partial^2 B_y}{\partial x^2} - \mu_{yy} \frac{\partial^2 B_y}{\partial y^2}. \end{aligned} \tag{16}$$

Neither condition generally holds in an FCT calculation, however, particularly the interchange of derivatives, since the flux F_z^a at each edge must be limited independently. Thus, the effect of the second contributions in Eqs. (15) may not be "antidiffusive" at all, and they have the potential to introduce severe numerical errors into the final solution (cf. Book *et al.* [2]). Put another way, there is no necessary relationship, in sign or magnitude, between the two contributions to the flux F_z^a in Eq. (14), and thus in their effects on the field components. They may oppose or reinforce each other, or one may overwhelm the other. In the latter case especially,

the flux-corrector would sharply reduce the flux to guard against generating or amplifying extrema in the smaller field component, producing a locally low-order, diffusive solution.

A considerable amount of experimentation has culminated in an alternative flux-corrector for the hydromagnetic equation which circumvents these difficulties. It is not as restrictive as that for the continuity equation, but still approximately enforces the monotonicity constraint on the magnetic field. The modified procedure is as follows:

(a) At each interface, calculate low-order solutions and establish extrema for the normal component of the field, ignoring any contributions by the transverse field component(s). In two dimensions, e.g., the extrema for B_x might be calculated from

$$\begin{aligned} \tilde{B}_{x\ i+1/2j} &= \max(B^o_{x\ i+1/2j},\ B^{lx}_{x\ i+1/2j}), \\ B^{\max}_{x\ i+1/2j} &= \max(\tilde{B}_{x\ i+1/2j-1},\ \tilde{B}_{x\ i+1/2j},\ \tilde{B}_{x\ i+1/2j+1}), \end{aligned} \tag{17}$$

where B^{lx}_x is the low-order solution calculated with only B_x-dependent terms included, and from analogous expressions for $B^{\min}_{x\ i+1/2j}$. The extrema for B_y would be established similarly.

(b) Cancel the downstream-directed, partial antidiffusive fluxes for each field component separately,

$$F^{ax}_{z\ i+1/2j+1/2} = 0 \qquad \text{if} \quad F^{ax}_{z\ i+1/2j+1/2}(B^{lx}_{x\ i+1/2j+1} - B^{lx}_{x\ i+1/2j}) < 0$$

and

$$F^{ax}_{z\ i+1/2j+1/2}(B^{lx}_{x\ i+1/2j+2} - B^{lx}_{x\ i+1/2j+1}) < 0 \tag{18}$$

or

$$F^{ax}_{z\ i+1/2j+1/2}(B^{lx}_{x\ i+1/2j} - B^{lx}_{x\ i+1/2j-1}) < 0,$$

where only the B_x-dependent terms are included in the antidiffusive fluxes F^{ax}_z.

(c) Calculate the inward- and outward-going partial antidiffusive fluxes for each interface,

$$\begin{aligned} P^{x+}_{i+1/2j} &= \max(F^{ax}_{z\ i+1/2j-1/2},\ 0) - \min(F^{ax}_{z\ i+1/2j+1/2},\ 0), \\ P^{x-}_{i+1/2j} &= \max(F^{ax}_{z\ i+1/2j+1/2},\ 0) - \min(F^{ax}_{z\ i+1/2j-1/2},\ 0). \end{aligned} \tag{19}$$

(d) Determine the maximum fractions of the partial fluxes which can be applied without causing overshoots or undershoots in the normal field component,

$$\begin{aligned} R^{x+}_{i+1/2j} &= \min(1,\ Q^{x+}_{i+1/2j}/P^{x+}_{i+1/2j}), \\ R^{x-}_{i+1/2j} &= \min(1,\ Q^{x-}_{i+1/2j}/P^{x-}_{i+1/2j}), \end{aligned} \tag{20}$$

where the maximum allowed fluxes into and out of the interface, respectively, are

$$\begin{aligned} Q^{x+}_{i+1/2j} &= (B^{\max}_{x\,i+1/2j} - B^{lx}_{x\,i+1/2j})\, A_{x\,i+1/2j}, \\ Q^{x-}_{i+1/2j} &= (B^{lx}_{x\,i+1/2j} - B^{\min}_{x\,i+1/2j})\, A_{x\,i+1/2j}. \end{aligned} \tag{21}$$

(e) At each edge, find the minimum fraction which prevents both an overshoot in the downstream interface and an undershoot in the upstream interface, for each field component separately,

$$C^{x}_{z\,i+1/2j+1/2} = \begin{cases} \min(R^{x+}_{i+1/2j+1}, R^{x-}_{i+1/2j}), & \text{if } F^{ax}_{z\,i+1/2j+1/2} \geqslant 0; \\ \min(R^{x+}_{i+1/2j}, R^{x-}_{i+1/2j+1}), & \text{otherwise.} \end{cases} \tag{22}$$

(f) Reduce the corresponding partial antidiffusive fluxes by these fractions, and combine the corrected partial fluxes to obtain the total corrected antidiffusive flux,

$$\begin{aligned} \tilde{F}^{ax}_{z\,i+1,2j+1/2} &= C^{x}_{z\,i+1/2j+1/2} F^{ax}_{z\,i+1/2j+1/2}, \\ \tilde{F}^{ay}_{z\,i+1/2j+1/2} &= C^{y}_{z\,i+1/2j+1/2} F^{ay}_{z\,i+1/2j+1/2}, \\ \tilde{F}^{a}_{z\,i+1/2j+1/2} &= \tilde{F}^{ay}_{z\,i+1/2j+1/2} - \tilde{F}^{ax}_{z\,i+1/2j+1/2}. \end{aligned} \tag{23}$$

For the purpose of obtaining the corrected antidiffusive fluxes, each component of the magnetic field is treated separately from the others. This avoids the problem encountered with the hydrodynamic flux-corrector, since each of the partial fluxes being corrected has a clearly "antidiffusive" effect on its associated field component. That the total fluxes constructed from these independently corrected, partial fluxes should yield a well-behaved final solution can be argued as follows. First, in regions where the velocity and magnetic fields are slowly varying, the antidiffusivities μ and correction coefficients C will be roughly uniform, so the interchange of numerical derivatives and thus Eqs. (16) will be approximately valid. In that case, the antidiffusive contributions by the transverse field components will just cancel a fraction of their diffusive contributions to the low-order solution $\mathbf{B}^l$. Neither of these contributions is considered by the flux-corrector, so the net effect will be the benign application of some additional, residual smoothing to each field component. Second, at a line or surface discontinuity, such as a shock front, the gradients along the coordinate normal to the discontinuity, x_n, are much greater than those along the transverse coordinate, x_t. Consequently, the ordering

$$\left|\frac{\partial B_t}{\partial t}\right| = \left|\frac{\partial F^a_z}{\partial x_n}\right| \gg \left|\frac{\partial F^a_z}{\partial x_t}\right| = \left|\frac{\partial B_n}{\partial t}\right|$$

will apply. Whatever correction of the partial antidiffusive flux F^{at}_z is necessary to ensure monotone behavior by its associated field component, B_t, can be applied without imposing a similarly abrupt change on the normal field component, B_n. At the same time, the partial flux F^{an}_z depends upon transverse gradients in the velocity

and magnetic fields and so makes only a small contribution in any event. Thus, situations in which $|\partial B_t/\partial x_n| \gg |\partial B_n/\partial x_t|$, precisely those that the hydrodynamic flux-corrector would deal with most restrictively, instead are handled effectively and accurately.

It is a straightforward matter to generalize this procedure to three spatial dimensions. In that case, the search for the extrema of $B_{x\ i+1/2jk}$ in Eq. (17) extends over the indices j and k of both transverse coordinates, with analogous formulae for B_y and B_z. The criterion of Eq. (18) for cancelling the downstream-directed, partial antidiffusive fluxes $F^{ax}_{z\ i+1/2j+1/2k}$, based on the variation of B^{lx}_x along y, is complemented by an identical condition on $F^{ax}_{y\ i+1/2jk+1/2}$ with respect to the variation of B^{lx}_x along z. Both pairs of modified fluxes, $F^{ax}_{y\ i+1/2jk\pm1/2}$ and $F^{ax}_{z\ i+1/2j\pm1/2k}$, then contribute to the total inward- and outward-going fluxes $P^x_{i+1/2jk}$ in Fig. (19). After the allowed interface fractions $R^x_{i+1/2jk}$ are determined from Eqs. (20) and (21), the correction factors $C^x_{z\ i+1/2j+1/2k}$ and $C^x_{y\ i+1/2jk+1/2}$ are calculated from Eq. (22) and its analogue. Finally, the total corrected antidiffusive flux $\tilde{F}^a_{y\ i+1/2jk+1/2}$ is obtained by combining the partial fluxes $\tilde{F}^{ax}_y$ and $\tilde{F}^{az}_y$ contributed by B_x and B_z, respectively, as is done for $\tilde{F}^a_{z\ i+1/2j+1/2k}$ in Eq. (23). The flux $\tilde{F}^a_{x\ ij+1/2k+1/2}$ is calculated similarly.

3. Examples

A flux-corrected transport algorithm for integrating generalized hydromagnetic equations in two spatial dimensions is described in the Appendix. I apply it here to some kinematical and dynamical problems of hydromagnetics. As an alternative to solving directly for the magnetic field, it is a common practice in MHD simulations to use a vector potential representation,

$$\mathbf{B} = \nabla \times \mathbf{A}, \tag{24}$$

whence the generalized hydromagnetic equation (1b) becomes

$$\frac{\partial \mathbf{A}}{\partial t} = \mathbf{v} \times \nabla \times \mathbf{A} + \mathbf{s}_5. \tag{25}$$

In two dimensions, only the component of the potential along the symmetry direction is needed, and Eq. (25) can be reduced to

$$\frac{\partial \psi}{\partial t} + \mathbf{v} \cdot \nabla \psi = \tilde{s}_5, \tag{26}$$

where the flux function ψ is a product of the symmetry component of $\mathbf{A}$ and a coordinate-system-dependent geometrical factor. The flux function is a convenient primitive variable, because algorithms for generalized continuity equations can be

modified to integrate advection equations such as Eq. (26). Also, it is a useful diagnostic since it can be shown that

$$\mathbf{B} \cdot \nabla \psi = 0, \tag{27}$$

i.e., surfaces of constant ψ are magnetic surfaces.

In the examples to follow, direct solutions of the ideal hydromagnetic equation (2) have been calculated using both the FCT field solver and an alternative monotone algorithm, the constrained transport (CT) scheme of Evans and Hawley [12]. They will be compared with each other and also with indirect solutions obtained by integrating Eq. (26) for the flux function, using a companion FCT fluid solver [13]. The discrete values of ψ are placed at the cell edges $(i+1/2, j+1/2)$, for consistency between the two calculations. The associated vector potential then is conservatively differenced to yield values of the magnetic-field components at the cell interfaces.

The first test is the rigid rotation of a current-carrying cylinder, analogous to Zalesak's [5, 6] slotted-cylinder test for fluid solvers. In cartesian coordinates, the flux function and the symmetry component of the vector potential are identical, $\psi = A_z$. Initial conditions for the calculation are shown in Fig. 2. The flux function, magnetic field, and current density within the cylinder are given by

$$\psi = \frac{r_0 B_0}{2}\left(1 - \frac{r^2}{r_0^2}\right),$$

$$B_\phi = \frac{r}{r_0} B_0,$$

$$J_z = \frac{2B_0}{r_0},$$

where (r, ϕ, z) is a cylindrical coordinate system centered on the cylinder of radius r_0 and peak field strength B_0. A sheath of return current at $r = r_0$ neutralizes the current carried in the interior, so that ψ, B_ϕ, and J_z vanish for $r > r_0$. The cylinder rotates rigidly in the counterclockwise direction at an angular rate ω, whence

where the origin of the cartesian coordinate system is placed on the axis of rotation. The calculations were performed on a 100×100 mesh, with the cylinder initially centered in the upper half plane and its radius set at 15 zones. The Courant number is 0.25, so that 1256 timesteps are required for one complete rotation.

The solutions obtained by the FCT field and potential solvers and the CT field solver are shown in the upper, center, and bottom panels, respectively, of Fig. 3. The errors in the flux functions, calculated from

$$\varepsilon = \frac{\sum_{i,j} |\psi^{\text{analytic}}_{i+1/2 j+1/2} - \psi^{\text{numeric}}_{i+1/2 j+1/2}|}{\sum_{i,j} |\psi^{\text{analytic}}_{i+1/2 j+1/2}|},$$

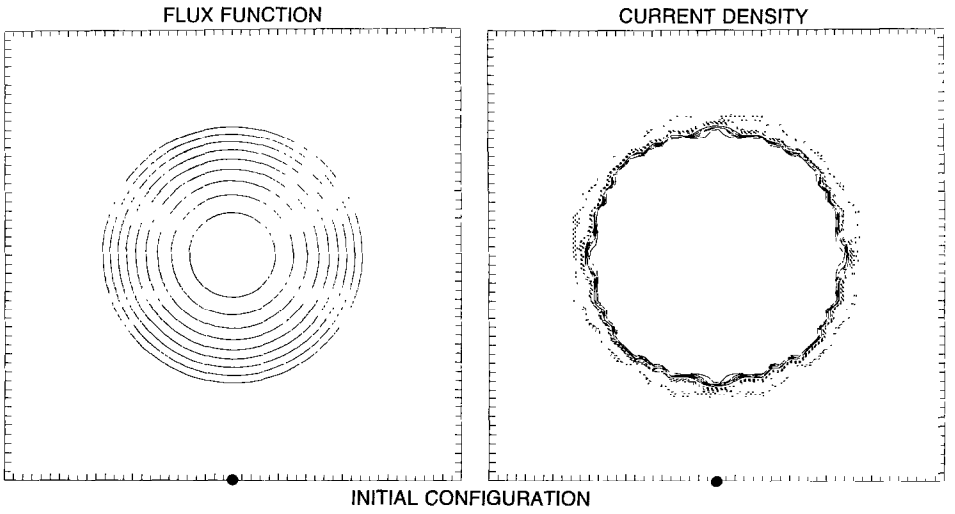

FIG. 2. The flux function $\psi = A_z$ (left) and current density J_z (right) for a rigid rotation test are displayed in their initial state. Only the 50×50 subdomain centered on the cylinder is shown, and the axis of rotation is marked by the solid dots. The flux function is contoured at 10%, 20%, ..., 90% of its peak initial value. The current density is contoured at $\pm 10\%$, $\pm 30\%$, ..., $\pm 90\%$ of its initial interior value, with positive percentages represented by the solid lines and negative percentages by the dashed lines.

are very small in the FCT cases, 6% for the field solver, 4% for the potential solver, and 14% for the CT field solver. Although the field solvers clearly preserve the symmetry of the flux surfaces better, yielding the better qualitative appearance, their solutions are somewhat more diffuse, which accounts for their lower quantitative accuracy. The truncation error of the CT algorithm is greater than that of the high-order FCT scheme, and that manifests itself in this quantitative comparison. The errors in the magnetic fields are essentially identical for the two FCT solvers at 25%, and 45% for the CT solver. For the field solvers, the error reflects the difficulty in advecting a discontinuous function—the magnetic field at $r = r_0$—using an Eulerian difference method. By way of comparison, an error of 24% results when Zalesak's slotted-cylinder test problem is solved using the FCT fluid solver [13]. For the potential solver, on the other hand, the error reflects the inaccuracies in the numerical derivatives of a smooth function—the vector potential—which has been accurately time-advanced by a monotonic scheme. The latter error is further amplified in the higher derivatives, sufficiently so that the potential solver yields a current density that is less accurate than does the FCT field solver, by 90% to 79%. The error in the diffuse current profile of the CT solution, for comparison, is 91%. Both FCT solutions for the current density show local depressions inside the cylinder, but the potential solver by far produces the more severe fluctuations, including a reversal near the axis of symmetry whose amplitude exceeds 70% of the initial interior value. The current density produced by the field solver is both qualitatively and quantitatively superior, although it again suffers in

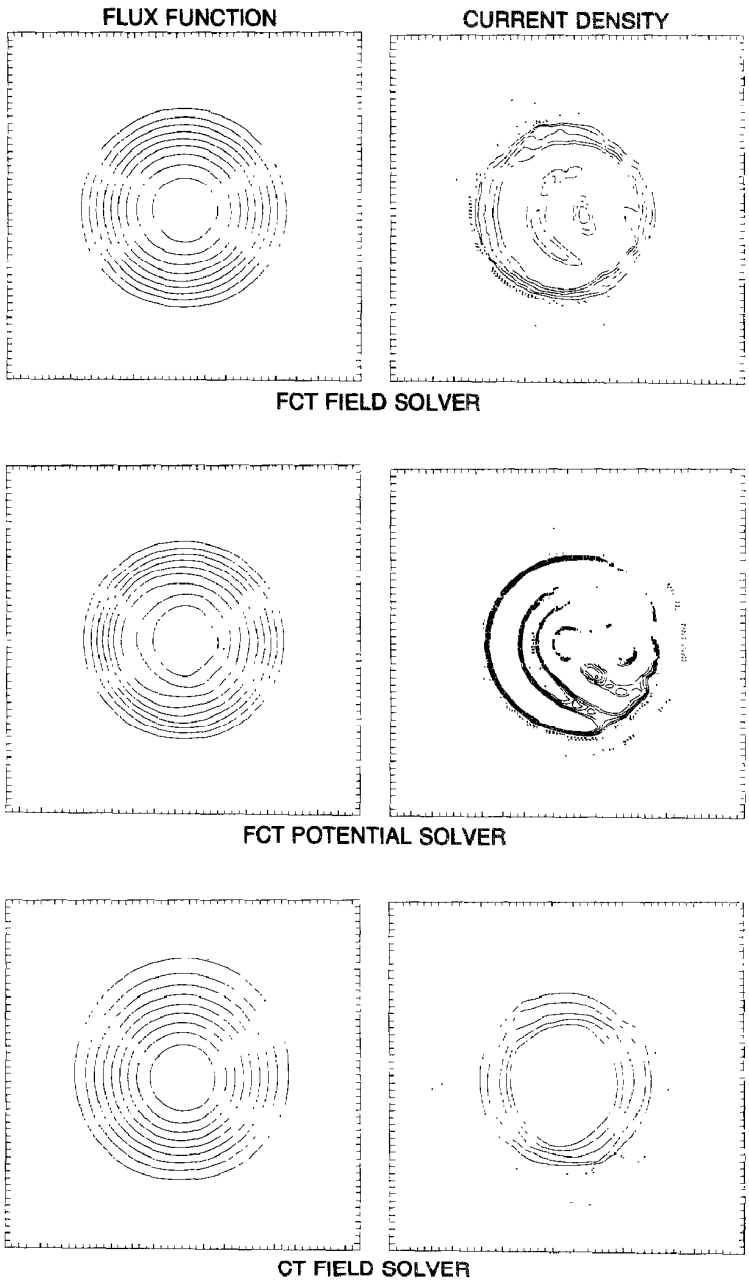

FIG. 3. The passively advected flux function $\psi = A_z$ (left) and current density J_z (right) are displayed in their final states produced by the new FCT solvers for the magnetic field (top) and vector potential (middle) and by the CT solver for the magnetic field (bottom). The contour levels are the same as those in the display of the initial state, Fig. 2.

the error comparison because its profile is not as sharp. The CT scheme smooths the current density even further, yielding the only monotonic profile, but the lowest quantitative accuracy, among the three solvers.

The second test is the self-similar spherical expansion of a strong shock wave and trailing magnetic bubble out of the gravitational well of a star, analyzed by Low [14, 15]. In this dynamical problem, the self-similar character of the expansion is maintained by a balance between pressure and magnetic forces in the colatitudinal direction and between pressure, magnetic, gravitational, and inertial forces in the radial direction. The simplest expansion is an inertial flow, whence

$$v_r(r, \theta, t) = r/t.$$

At time t_0, the shock and its associated contact surface coincide at radius r_0; at later times, their positions are given by

$$\frac{r_s(t)}{r_0} = \left(\frac{t}{t_0}\right)^{7/6},$$

$$\frac{r_c(t)}{r_0} = \left(\frac{t}{t_0}\right),$$

respectively. A magnetic bubble is embedded behind the contact surface, and the flux function $\psi = r \sin \theta A_\phi$ initially satisfies

$$\psi(r, \theta, t_0) = \begin{cases} \psi_0(r_2 - r)(r - r_1) \sin^2 \theta, & \text{if } r_1 < r < r_2; \\ 0, & \text{otherwise,} \end{cases}$$

for $r_1 = 0.55 r_0$ and $r_2 = 0.95 r_0$. The simulations were carried out for times $2t_0 \leqslant t \leqslant 5t_0$, on the spatial grid $r_0 \leqslant r \leqslant 5r_0$, $0 \leqslant \theta \leqslant \pi/2$. The 600 timesteps used correspond to an average Courant number of about 0.25, and the grid spacing on the 100×100 mesh increased linearly with r and was uniform in θ. A predictor/corrector integration method was used to time-center the source terms and achieve second-order accuracy in time. Finally, the gravitational parameter GMt_0^2/r_0^3 was assigned the special value $\frac{2}{3}$, for which both the mass density and the pressure are continuous across the contact surface, and the flux constant ψ_0 was chosen to yield a minimum plasma β (ratio of plasma to magnetic pressure) of unity.

The flux surfaces at the initial and final times are shown in the upper panel of Fig. 4. Shown in the center panel are the solutions produced by the FCT field and potential solvers, and shown in the lower panel is the CT solution. They are quite similar, both qualitatively and quantitatively, although the field solvers yield noticeably smoother flux surfaces. The errors in the flux function are nearly identical for the three solvers, at 8–9 %. The errors in the field components also are essentially equal for the FCT solvers (20%), and the error for the slightly more diffuse CT solution is somewhat larger (25%). As in the passive advection test, the FCT potential solver yields a less accurate current density than the FCT field solver, by

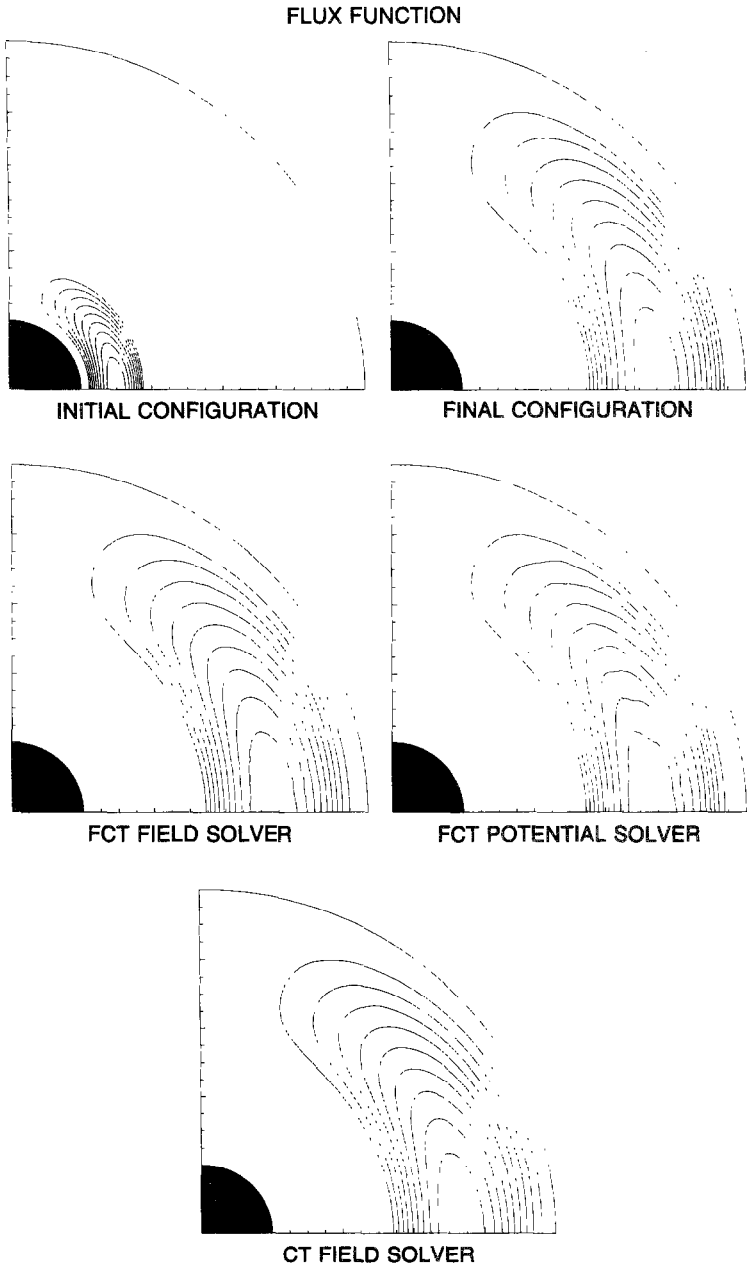

FIG. 4. The flux function $\psi = r \sin \theta A_\phi$ for a self-similar spherical expansion of a magnetic bubble embedded in a stellar envelope is displayed, in its initial and exact final states (top) and in the final states produced by the FCT solvers (middle) and the CT solver (bottom). The domain $r_0 \leqslant r \leqslant 5r_0$, $0 \leqslant \theta \leqslant \pi/2$ is shown as projected against the sky; the shaded region is $r \leqslant r_0$. The flux function is contoured at 10%, 20%, ..., 90% of its peak initial value.

errors of 113% to 88%. Both solvers produce local current reversals in this problem, however—the potential solver at the 90% level and the field solver at the 10% level. The smoother current density produced by the CT solver also is in error by 88%. Contour plots of the current densities in this problem are not shown because they are not very instructive; numerically generated small-scale structures dominate the current distribution within the magnetic bubble.

4. Discussion

A conservative integration of the generalized hydromagnetic equation of magnetohydrodynamics is readily effected by defining the components of the magnetic field at the interfaces of the finite-difference grid. The convective and other fluxes whose application causes the magnetic field to evolve in time are defined at the cell edges. Because each such flux affects four discrete field values along two coordinate directions, the calculation is inherently multidimensional—an operator-split integration for the individual field components is necessarily nonconservative. This characteristic distinguishes the hydromagnetic equation from the continuity equation, which can be integrated as conservatively, though not as accurately, in an operator-split approach as in a fully multidimensional formulation.

To successfully apply FCT techniques to the integration of the hydromagnetic equation does require, however, that operator-splitting techniques be employed by the flux-corrector. The contributions of each field component to the antidiffusive fluxes must be computed and corrected individually, rather than jointly. Otherwise, the fluxes tend to be severely limited, producing a diffuse, inaccurate solution. The monotonicity constraint clearly cannot be strictly enforced by any flux-corrector which splits the antidiffusive fluxes in this way. Nevertheless, the numerical examples demonstrate that an accurate solution can be obtained, far superior in particular to that provided by either the low- or high-order scheme used alone.

The FCT field solver holds a small advantage over both the FCT potential solver and the constrained transport (CT) scheme [12] in the quantitative accuracy to which the flux surfaces and field strengths are reproduced, in the numerical tests discussed. Its solutions also possess superior symmetry and smoothness properties and the quantitative accuracy of its electric-current distributions is higher, certainly by comparison with the potential solver, though only marginally so with respect to the CT field solver. Contrary to what might be expected, in the dynamical tests cited the differences in the accuracy of the current distributions does not translate into substantially different flux-surface or field-strength errors. This outcome may be due to the rather high plasma β and short elapsed time in these simulations, in which the Lorentz force does not play a dominant role and differences between the two solutions do not accumulate over many timesteps. In lengthy simulations of the evolution of low-β plasmas, on the other hand, the direct solution for the magnetic field may be more clearly preferable.

It should be kept in mind that using FCT to evolve the magnetic field in an MHD calculation generally will produce some dissipation of magnetic flux. The numerical diffusion in the scheme acts much like a physical resistivity. Prime dissipation sites are the locations of discontinuities in the field, i.e., current sheets, where the flux-corrector may severely limit the antidiffusive fluxes to keep the solution monotonic. The rate of dissipation is determined by the amount of flux correction that is done, and thus depends sensitively upon the details of the field and flow patterns and upon the rule for establishing the solution's allowed extrema. A generally useful rule was given in Eq. (17) and used in the numerical examples in this paper, but other, equally well motivated criteria could be imposed instead (cf. [5]). In any case, the less restrictive is the rule used, the lower is the dissipation rate, but the noisier are the solutions that result.

The developments of flux-corrected transport described in this paper were motivated by an interest in numerical simulation of MHD shocks and blast waves and general supersonic, magnetized flows. For these applications, the dissipation inherent in the scheme is used to advantage, to prevent the formation of unphysical ripples in the vicinity of discontinuities in the magnetic field. For application to other problems, such as the development of MHD instabilities, evolution of MHD turbulence, or basic studies of magnetic reconnection, the suitability of FCT depends upon several factors. These include the accuracy of the high-order scheme, which governs the dependence of the minimum dissipation rate on the grid spacing and timestep; the specifics of the flux-corrector, which determines the amount of dissipation that is retained, as discussed above; and the spatial and temporal resolution employed in the calculation, which finally fix the numerical dissipation rates. In principle, the methods described herein could be used to investigate any of these magnetohydrodynamic phenomena, although alternative methods may be more ideally suited for certain applications.

APPENDIX

I present here an efficient, accurate algorithm for integrating the generalized hydromagnetic equation of two-dimensional, compressible magnetohydrodynamics. This algorithm employs the flux-corrected transport techniques developed previously for multidimensional hydrodynamics, and extended in this paper to magnetohydrodynamical problems. In the course of the calculation, intermediate low-order solutions B_x^{lx} and B_y^{ly}, to which only the B_x- and B_y-dependent fluxes contribute, respectively, are needed. These solutions are not divergence-free, but they are used solely to correct their associated partial antidiffusive fluxes F_z^{ax} and F_z^{ay}. After correction, these partial fluxes are combined to obtain the total antidiffusive flux $\tilde{F}_z^a$, which in turn is used in the final step to generate the divergence-free solution $\mathbf{B}_f$.

The calculation consists of convection, diffusion, and antidiffusion stages. In the convection stage, there results

$$\begin{aligned}
B^{cy}_{x\,i+1/2j} A_{x\,i+1/2j} &= B^{o}_{x\,i+1/2j} A_{x\,i+1/2j} + F^{cx}_{z\,i+1/2j-1/2} - F^{cx}_{z\,i+1/2j+1/2},\\
B^{cx}_{y\,ij+1/2} A_{y\,ij+1/2} &= B^{o}_{y\,ij+1/2} A_{y\,ij+1/2} + F^{cy}_{z\,i-1/2j+1/2} - F^{cy}_{z\,i+1/2j+1/2};\\
B^{c}_{x\,i+1/2j} A_{x\,i+1/2j} &= B^{o}_{x\,i+1/2j} A_{x\,i+1/2j} - F^{c}_{z\,i+1/2j-1/2} + F^{c}_{z\,i+1/2j+1/2},\\
B^{c}_{y\,ij+1/2} A_{y\,ij+1/2} &= B^{o}_{y\,ij+1/2} A_{y\,ij+1/2} + F^{c}_{z\,i-1/2j+1/2} - F^{c}_{z\,i+1/2j+1/2}.
\end{aligned} \tag{A1}$$

The convective fluxes due to B_x and B_y separately and jointly are given, respectively, by

$$\begin{aligned}
F^{cx}_{z\,i+1/2j+1/2} &= B^{o}_{x\,i+1/2j+1/2} L_{z\,i+1/2j+1/2} v_{y\,i+1/2j+1/2}\,\Delta t,\\
F^{cy}_{z\,i+1/2j+1/2} &= B^{o}_{y\,i+1/2j+1/2} L_{z\,i+1/2j+1/2} v_{x\,i+1/2j+1/2}\,\Delta t,\\
F^{c}_{z\,i+1/2j+1/2} &= F^{cy}_{z\,i+1/2j+1/2} - F^{cx}_{z\,i+1/2j+1/2},
\end{aligned} \tag{A2}$$

where the edge magnetic fields are calculated as the averages

$$\begin{aligned}
B^{o}_{x\,i+1/2j+1/2} &= \tfrac{1}{2}(B^{o}_{x\,i+1/2j} + B^{o}_{x\,i+1/2j+1}),\\
B^{o}_{y\,i+1/2j+1/2} &= \tfrac{1}{2}(B^{o}_{y\,ij+1/2} + B^{o}_{y\,i+1j+1/2}).
\end{aligned}$$

The diffusion stage ensures the monotonicity of the low-order solution,

$$\begin{aligned}
B^{dy}_{x\,i+1/2j} A_{x\,i+1/2j} &= B^{cy}_{x\,i+1/2j} A_{x\,i+1/2j} + F^{dx}_{z\,i+1/2j-1/2} - F^{dx}_{z\,i+1/2j+1/2},\\
B^{dx}_{y\,ij+1/2} A_{y\,ij+1/2} &= B^{cx}_{y\,ij+1/2} A_{y\,ij+1/2} + F^{dy}_{z\,i-1/2j+1/2} - F^{dy}_{z\,i+1/2j+1/2},\\
B^{d}_{x\,i+1/2j} A_{x\,i+1/2j} &= B^{c}_{x\,i+1/2j} A_{x\,i+1/2j} - F^{d}_{z\,i+1/2j-1/2} + F^{d}_{z\,i+1/2j+1/2},\\
B^{d}_{y\,ij+1/2} A_{y\,ij+1/2} &= B^{c}_{y\,ij+1/2} A_{y\,ij+1/2} + F^{d}_{z\,i-1/2j+1/2} - F^{d}_{z\,i+1/2j+1/2},
\end{aligned} \tag{A3}$$

where the diffusive fluxes are given by

$$\begin{aligned}
F^{dx}_{z\,i+1/2j+1/2} &= v_{yy\,i+1/2j+1/2}(B^{o}_{x\,i+1/2j} - B^{o}_{x\,i+1/2j+1})\,A_{x\,i+1/2j+1/2},\\
F^{dy}_{z\,i+1/2j+1/2} &= v_{xx\,i+1/2j+1/2}(B^{o}_{y\,ij+1/2} - B^{o}_{y\,i+1j+1/2})\,A_{y\,i+1/2j+1/2},\\
F^{d}_{z\,i+1/2j+1/2} &= F^{dy}_{z\,i+1/2j+1/2} - F^{dx}_{z\,i+1/2j+1/2}.
\end{aligned} \tag{A4}$$

For the diffusion along x, the coefficient is

$$v_{xx\,i+1/2j+1/2} = \tfrac{1}{6} + \tfrac{1}{3}\varepsilon^2_{x\,i+1/2j+1/2}, \tag{A5}$$

the signed Courant number is

$$\varepsilon_{x\,i+1/2j+1/2} = \frac{1}{2}\left(\frac{1}{A_{y\,ij+1/2}} + \frac{1}{A_{y\,i+1j+1/2}}\right) v_{x\,i+1/2j+1/2} L_{z\,i+1/2j+1/2}\,\Delta t,$$

and the edge area is the average

$$A_{y\,i+1/2j+1/2} = \tfrac{1}{2}(A_{y\,ij+1\,2} + A_{y\,i+1j+1/2}).$$

Analogous definitions apply along y. Adding the contributions of the source term yields the low-order solution,

$$\begin{aligned}
B^{lx}_{x\,i+1/2j} A_{x\,i+1/2j} &= B^{dy}_{x\,i+1/2j} A_{x\,i+1/2j} - F^{s}_{z\,i+1\,2j-1/2} + F^{s}_{z\,i+1/2j+1/2},\\
B^{ly}_{y\,ij+1/2} A_{y\,ij+1/2} &= B^{dx}_{y\,ij+1/2} A_{y\,ij+1/2} + F^{s}_{z\,i-1/2j+1\,2} - F^{s}_{z\,i+1/2j+1/2};\\
B^{l}_{x\,i+1/2j} A_{x\,i+1/2j} &= B^{d}_{x\,i+1\,2j} A_{x\,i+1\,2j} - F^{s}_{z\,i+1/2j-1/2} + F^{s}_{z\,i+1\,2j+1/2},\\
B^{l}_{y\,ij+1\,2} A_{y\,ij+1/2} &= B^{d}_{y\,ij+1\,2} A_{y\,ij+1/2} + F^{s}_{z\,i-1\,2j+1\,2} - F^{s}_{z\,i+1\,2j+1/2},
\end{aligned} \tag{A6}$$

where

$$F^{s}_{z\,i+1/2j+1/2} = \Delta t L_{z\,i+1/2j+1/2} s_{4z\,i+1/2j+1/2}$$

is the edge flux due to the source term $\mathbf{s}_4$.

The high-order solutions are given by

$$\begin{aligned}
B^{h}_{x\,i+1/2j} A_{x\,i+1/2j} &= B^{l}_{x\,i+1/2j} A_{x\,i+1/2j} - F^{a}_{z\,i+1\,2j-1/2} + F^{a}_{z\,i+1/2j+1\,2},\\
B^{h}_{y\,ij+1/2} A_{y\,ij+1/2} &= B^{l}_{y\,ij+1/2} A_{y\,ij+1/2} + F^{a}_{z\,i-1/2j+1\,2} - F^{a}_{z\,i+1\,2j+1/2}.
\end{aligned} \tag{A7}$$

The partial and total uncorrected antidiffusive fluxes are

$$\begin{aligned}
F^{ax}_{z\,i+1/2j+1/2} &= \mu_{yy\,i+1/2j+1/2}(B^{cy}_{x\,i+1/2j+1} - B^{cy}_{x\,i+1\,2j}) A_{x\,i+1/2j+1/2}\\
&\quad + \mu_{yx\,i+1/2j+1/2}(B^{cy}_{x\,i+1j+1\,2} - B^{cy}_{x\,ij+1\,2}) A_{x\,i+1/2j+1/2},\\
F^{ay}_{z\,i+1/2j+1/2} &= \mu_{xx\,i+1/2j+1\,2}(B^{cx}_{y\,i+1j+1\,2} - B^{cx}_{y\,ij+1\,2}) A_{y\,i+1/2j+1\,2}\\
&\quad + \mu_{xy\,i+1/2j+1/2}(B^{cx}_{y\,i+1\,2j+1} - B^{cx}_{y\,i+1\,2j}) A_{y\,i+1/2j+1/2},\\
F^{a}_{z\,i+1\,2j+1/2} &= F^{ay}_{z\,i+1/2j+1/2} - F^{ax}_{z\,i+1/2j+1/2},
\end{aligned} \tag{A8}$$

where the coefficients for antidiffusion along x are

$$\begin{aligned}
\mu_{xx\,i+1/2j+1/2} &= \tfrac{1}{6} - \tfrac{1}{6}\varepsilon^2_{x\,i+1\,2j+1/2},\\
\mu_{xy\,i+1/2j+1/2} &= -\tfrac{1}{2}\varepsilon_{x\,i+1/2j+1\,2}\varepsilon_{y\,i+1/2j+1/2}.
\end{aligned} \tag{A9}$$

The convected solution for B_x at the y interfaces is calculated as the average

$$B^{cx}_{x\,ij+1/2} = \tfrac{1}{4}(B^{cx}_{x\,i-1/2j} + B^{cx}_{x\,i-1/2j+1} + B^{cx}_{x\,i+1\,2j} + B^{cx}_{x\,i+1/2j+1}).$$

The coefficients for antidiffusion along y and the convected solution for B_y at the x interfaces are calculated similarly.

The partial antidiffusive fluxes of Eq. (A8) now are corrected using the prescription of Section 2, Eqs. (17–(22) for B_x, and their analogues for B_y. These corrected

partial fluxes are combined according to Eq. (23) and then applied to the low-order solutions of Eq. (A6),

$$\begin{aligned} B^f_{x\ i+1/2j} A_{x\ i+1/2j} &= B^l_{x\ i+1/2j} A_{x\ i+1/2j} - \tilde{F}^a_{z\ i+1/2j-1/2} + \tilde{F}^a_{z\ i+1/2j+1/2}, \\ B^f_{y\ ij+1/2} A_{y\ ij+1/2} &= B^l_{y\ ij+1/2} A_{y\ ij+1/2} + \tilde{F}^a_{z\ i-1/2j+1/2} - \tilde{F}^a_{z\ i+1/2j+1/2}. \end{aligned} \tag{A10}$$

This is the desired solution to the generalized hydromagnetic equation (1).

For the special case of uniform advection of magnetic flux over a uniform, cartesian mesh, a complete error and stability analysis of the algorithm can be carried out. The phase and amplitude errors of the low-order solution, Eq. (A6), are second order in the grid spacing at long wavelengths, and the scheme is absolutely stable for Courant numbers $|\varepsilon_{x,y}| < \frac{1}{2}$. The errors in the high-order solution, Eq. (A7), are fourth order.

ACKNOWLEDGMENTS

I benefitted significantly from insights and encouragement offered by both developers and users of flux-corrected transport methods among my colleagues at the Naval Research Laboratory. Financial support was provided by the Office of Naval Research through the Naval Research Laboratory (JO 44-1527-0-7, 8, 9) and by the National Acronautics and Space Administration (Solar Terrestrial Theory Program).

REFERENCES

1. J. P. BORIS AND D. L. BOOK, *J. Comput. Phys.* **11**, 38 (1973).
4. J. P. BORIS, Naval Research Laboratory Memorandum Report No. 3237, 1976 (unpublished).
5. S. T. ZALESAK, *J. Comput. Phys.* **31**, 335 (1979).
6. D. L. BOOK, J. P. BORIS, AND S. T. ZALESAK, "Flux-Corrected Transport," *Finite-Difference Techniques for Vectorized Fluid Dynamics Calculations*, edited by D. L. Book (Springer-Verlag, New York, 1981), p. 29.
7. R. H. GUIRGUIS, JAYCOR Report No. J206-83-003/6201, 1983 (unpublished).
8. G. PATNAIK, R. H. GUIRGUIS, J. P. BORIS, AND E. S. ORAN, *J. Comput. Phys.* **71**, 1 (1987).
9. R. LÖHNER, K. MORGAN, M. VAHDATI, J. P. BORIS, AND D. L. BOOK, *Commun. Appl. Num. Methods* **4**, 717 (1988).
10. S. T. ZALESAK, Plasma Physics Division, Naval Research Laboratory, Washington, DC, private communication (1987).
11. D. SCHNACK AND J. KILLEEN, *J. Comput. Phys.* **35**, 110 (1980).
12. C. R. EVANS AND J. F. HAWLEY, *Astrophys. J.* **332**, 659 (1988).
13. C. R. DEVORE, Naval Research Laboratory Memorandum Report No. 6544, 1989 (unpublished).
14. B. C. LOW, *Astrophys. J.* **281**, 381 (1984).
15. B. C. LOW, *Astrophys. J.* **281**, 392 (1984).